Effect of Plasma-Sprayed Alumina on the Strength, Elastic Modulus, and Damping of Ti-25Al-10Nb-3V-1Mo Intermetallic

R.U. Vaidya, A.K. Zurek, A. Wolfenden, D.A. Bowles, and M.W. Cantu

The effect of a plasma-sprayed Al_2O_3 coating on the bend strength, elastic modulus, and damping of Ti-25Al-10Nb-3V-1Mo intermetallic substrate was measured. Two coating thicknesses of 0.1 and 1.0 mm were used in the study. The average strength and Weibull coefficients of the intermetallic samples coated with the 0.1 mm Al_2O_3 coating were very similar to those of the uncoated intermetallic samples. On the other hand, the average strength of the samples coated with 1.0 mm Al_2O_3 was significantly lower than the strength of the uncoated intermetallic substrate. The lower strength of the 1.0 mm coated samples was attributed to the higher volume fraction of the Al_2O_3 coating (which has a lower strength than the Ti-25Al-10Nb-3V-1Mo substrate) and higher porosity in the 1.0 mm coating. The Young's modulus and damping values of the 0.1 mm Al_2O_3-coated intermetallics did not vary significantly from those of the uncoated substrate. However, the damping values of the 1.0 mm Al_2O_3-coated intermetallics were significantly larger than those of the uncoated substrate. The higher damping values measured for the 1.0 mm Al_2O_3-coated samples were attributed to the higher porosity in the thicker coating and to defects in the coating as a result of the spraying process.

Keywords

alumina, plasma spray, Ti-Al-Nb-V-Mo intermetallic, Weibull analysis

1. Introduction

PLASMA-SPRAYED ceramic coatings are commonly applied to metal or ceramic substrates in order to provide chemical and/or thermal protection in high-temperature corrosive environments. They also have the potential to provide high-temperature oxidation resistance to Ti-Al intermetallics. If such intermetallics are left unprotected, oxidation occurring at elevated temperatures can severely degrade their mechanical properties. The problem of elevated-temperature oxidation has to be addressed in applications involving such intermetallics because of the high cost and complexity involved in the manufacture of these materials.

Our study addresses some of the issues relevant to the development of an alumina coating for Ti-25Al-10Nb-3V-1Mo intermetallic substrate. Physical and mechanical properties of the intermetallic substrate and alumina coating are listed in Table 1. The strength of the intermetallic at elevated temperatures decreases only slightly from its room-temperature strength value, while its ductility and fracture toughness increase significantly with increasing temperatures. The intermetallic, however, suffers from significant surface oxidation at temperatures in excess of 600 °C. The primary oxide layer (TiO_{2-x}, $x < 0.01$) formed on the surface of the uncoated intermetallic does not adhere well to the substrate, and as a result the oxidation process continues and leads to degradation of the substrate.

R.U. Vaidya and **A.K. Zurek,** Materials Science and Technology, Los Alamos National Laboratory, Los Alamos, NM 87545, USA; and **A. Wolfenden, D.A. Bowles,** and **M.W. Cantu,** Department of Mechanical Engineering, Texas A and M University, College Station, TX 77843, USA.

There are three main factors to be considered in the selection of the appropriate coating material: chemical, mechanical, and thermal compatibility. Additionally, the cost of the coating material and the cost and ease of applying the coating material to the substrate should be considered in the selection process. Alumina is a good choice as a coating material because of its low cost, availability, and adaptability to the plasma spraying process. We have shown in previous studies (Ref 1, 2) that alumina is chemically, mechanically, and thermally compatible with the Ti-25Al-10Nb-3V-1Mo intermetallic. An alumina coating applied to the surface of the intermetallic was effective as an oxidation barrier at elevated temperatures. The alumina coating bonded mechanically with the intermetallic substrate, and no elemental diffusion occurred across the coating/substrate interface, even when the coated samples were exposed to temperatures as high as 1000 °C for an extended period of time. The thermal stresses induced at the coating/substrate interface were small due to the small difference in the coefficient of thermal expansion between the coating and substrate. We observed that the coating applied did not spall off with repeated thermal cycling between 1000 °C and room temperature. However,

Table 1 Physical and mechanical properties of the substrate and coating as cited in literature

Property	Ti-25Al-10Nb-3V-1Mo	Al_2O_3
Density, g/cm^3	4.3	3.96 (max)
Young's modulus, GPa	125	320
Tensile strength, MPa	1042	200-345
Oxidation limit, °C	650	...
Ductility at RT, %	2-10	...
Ductility at HT, %	10-20	...
Coefficient of thermal expansion, 10^{-6} °C^{-1}	10 10 RT to 1000 °C	8.9 RT to 1000 °C 8.9

RT, room temperature; HT, high temperature

Table 2 Chemical composition of the intermetallic substrate

Elements	Ti	Al	Nb	V	Mo	Cu	Si	Fe
wt%	56.3	14	23.4	3.87	2.07	0.15	0.1	0.08
at.%	60.8	25	10	3	1	(a)	(a)	(a)

(a) Trace concentrations

cracking was observed in the region of the coating adjacent to the coating/substrate interface.

Such coatings applied to the surface of intermetallics can significantly affect the strength and elastic modulus of the intermetallics, since the fracture characteristics of the coating and substrate materials are greatly different. In our present study we have primarily focused on studying the effect of the plasma-sprayed alumina coatings on the bending strength, elastic modulus, and damping of the Ti-25Al-10Nb-3V-1Mo intermetallic substrate. The effect of the coating thickness on these properties was determined. Differences in the fracture characteristics of the coated and uncoated materials were compared and contrasted through fractographic examinations.

2. Materials and Coating Procedure

The Ti-25Al-10Nb-3V-1Mo intermetallic substrates used in the study were obtained in the form of cast plates from Howmet Inc. The chemical composition of the plates as determined by wavelength dispersive spectroscopy is given in Table 2. Small samples (40 × 40 × 3 mm) were cut out from the larger intermetallic plates before spraying.

The alumina coatings were applied to the substrate by plasma spraying. The bonding between the plasma-sprayed alumina coating and Ti-25Al-10Nb-3V-1Mo substrate was determined to be mechanical in nature, so sand blasting of the intermetallic coupons was carried out prior to spraying. Sand blasting roughens the surface of the intermetallic, and it enhances the bonding between the coating and substrate by providing large interlocking sites. Alumina powder (Metco 105) was used for the spraying process. The powder also contained 0.3 wt% silica. A Plasmadyne (Miller Thermal Inc., Appleton, WI) gun was used for spraying the alumina onto the intermetallic substrate. The plasma spraying parameters used were:

- *Plasma gun voltage:* 25 V
- *Plasma gun current:* 300 A
- *Gun-to-specimen distance:* 7.5 cm
- *Arc and powder gas:* argon
- *Atmosphere:* air

Two different coating thicknesses of 0.1 and 1.0 mm were applied to the intermetallic in this study. Porosity in the coatings, as determined by image analysis, was an average of 4.3% for the 0.1 mm coatings and 7.8% for the 1.0 mm coatings.

3. Experimental Procedure

3.1 *Determination of Bend Strength*

The strength of the coated and uncoated intermetallic samples was measured in three-point bending. The samples were loaded in a hardened steel fixture and were supported on hardened steel pins at two points, 19 mm apart. Loading was accomplished by a central loading pin.

Samples were cut out of the uncoated and coated plates using a low-speed diamond saw. Although the dimensions varied slightly from sample to sample, the variation in the dimensions for one set of samples was small. The average ratios of the loading span to the specimen thickness (*L/d*), loading span to specimen width (*L/b*), and specimen width to specimen thickness (*b/d*) were as follows:

Specimen	*L/d*	*L/b*	*b/d*
Uncoated	9.60	4.9	1.96
0.1 mm coating	9.22	5.7	1.61
1.0 mm coating	4.8	3.8	1.26

The maximum stress in the samples was calculated using the equation

$$S = 3pL/2bd^2 \quad \text{(Eq 1)}$$

where S is the maximum stress in the sample, p is the maximum load at which the sample fractured, L is the support span length, b is the width of the sample, and d is the sample thickness.

The samples were loaded in an Instron™ machine (Instron Corporation, Canton, MA) equipped with a 5 kN load cell and were tested at a crosshead speed of 0.1 mm/min.

A Weibull statistical approach (Ref 3) was used to obtain the strength distributions in the coated and uncoated samples. The Weibull approach is based on the weakest link theory and gives the probability of failure P at stress σ_f as:

$$P(\sigma_f) = 1 - \exp\left[-V_E((\sigma_f - \sigma_u)/\sigma_0)^\beta\right. \quad \text{(Eq 2)}$$

Here, V_E is the effective sample volume under stress, a function of the sample size and testing configuration; σ_0 is a scale parameter; σ_u is the stress below which the probability of failure is zero; and β is the Weibull modulus. The Weibull modulus is an important parameter in characterizing the strength of brittle materials, and it is a measure of the scatter in the strength of the material. Also, the Weibull modulus is required to extrapolate data in order to predict the probability of failure of larger or smaller volumes of material under an applied stress.

Taking a conservative estimate of σ_u equal to zero, Eq 2 can be simplified to a two-parameter distribution as:

$$P(\sigma_f) = 1 - \exp[-\alpha\sigma_f^\beta] \quad \text{(Eq 3)}$$

where α is the modified scale parameter (equal to V_E/σ_0^β).

Taking the natural logarithm of Eq 3 twiceand rearranging, we get:

$$\ln\ln[1/(1-P)] = \ln\alpha + \beta\ln\sigma_f \quad \text{(Eq 4)}$$

By plotting $\ln\ln[1/(1-P)]$ against $\ln\sigma_f$ one can obtain the Weibull modulus β. The probability of failure P is obtained by arranging the strength values of the samples in ascending order, then assigning a probability of failure to each strength value using an estimator given by:

$$P(\sigma_{fi}) = i/(1+N) \quad \text{(Eq 5)}$$

where $P(\sigma_{fi})$ gives the probability of failure corresponding to the i^{th} strength value, and N is the total number of samples tested.

The Weibull mean strength σ_f, standard deviation sd, and coefficient of variation CV are given by:

$$\sigma_f = \alpha^{-1/\beta}\Gamma[1 + 1/\beta] \quad \text{(Eq 6)}$$

$$\text{sd} = \alpha^{-1/\beta}[\Gamma 1 + {}^{2}/_{\beta}) - \Gamma^2(1 + {}^{1}/_{\beta})]^{1/2} \quad \text{(Eq 7)}$$

$$\text{CV} = 100\,\text{sd}/\sigma_f \quad \text{(Eq 8)}$$

where

$$\Gamma(n) = \int_0^\infty e^{-x}x^{n-1}dx$$

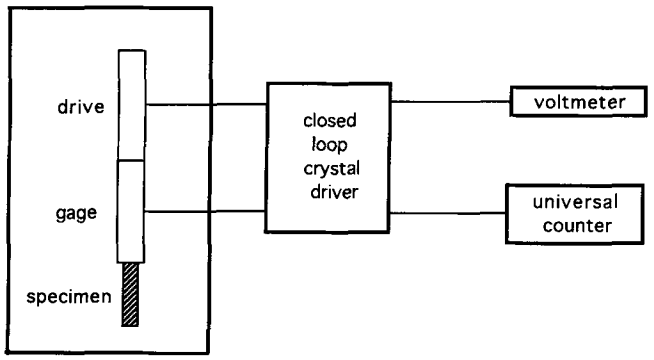

Fig. 1 Schematic of the PUCOT setup used for determining the Young's modulus and damping

3.2 *Determination of Elastic Modulus and Damping*

Samples for the elastic modulus and damping measurements were cut into sizes appropriate for the experiment. The dimensions and the mass density of the samples were measured prior to the experimentation. The piezoelectric ultrasonic composite oscillator technique (PUCOT) was used for measuring the elastic modulus and vibrational damping of the coated and uncoated samples. The apparatus consists of two piezoelectric quartz crystals, the drive D and gage G, and the specimen S. A schematic of the setup used can be seen in Fig. 1. The crystals are resonated at their natural frequency in the longitudinal mode at approximately 100 kHz. This is done by means of an alternating voltage applied to the drive crystal. For the measurements at room temperature, the specimen S of appropriate resonant length is glued to the end of the gage crystal. From the measurement of the mass and length of the various components, the mass density of the specimen, the resonant period of the D and G crystals, and the resonant period of the system (DGS), the values of the dynamic Young's modulus E, mechanical damping Q^{-1}, and strain amplitude are determined. Details of the experimental technique used have been provided elsewhere (Ref 4, 5). Damping measurements are sensitive to microcracks and other defects in the material, and they can be a useful tool in determining the integrity of the material system.

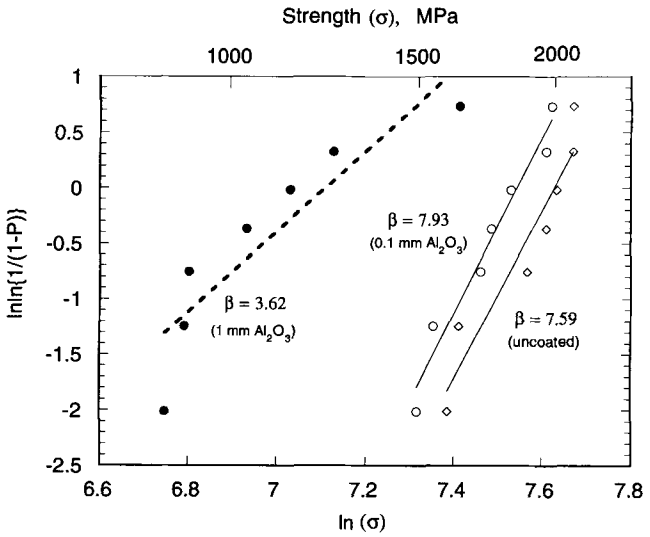

Fig. 2 Weibull strength distribution plot for the uncoated and coated intermetallic substrates

Table 3 Weibull parameters

Sample condition	α	β	Weibull mean strength, MPa	Standard deviation, MPa	Coefficient of variation, %	Correlation coefficient
Uncoated	7×10^{-26}	7.59	1751	291	16.6	0.95
0.1 mm Al_2O_3-coated	1×10^{-26}	7.93	1775	304	17.2	0.98
1 mm Al_2O_3-coated	6.5×10^{-12}	3.62	1098	343	31.2	0.90

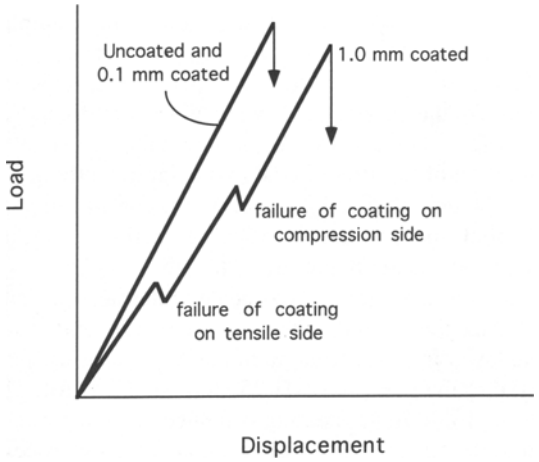

Fig. 3 Schematic of the load-displacement curves for the uncoated and coated intermetallic substrates

4. Results and Discussion

A summary of the bend strength and related Weibull statistical data for the uncoated intermetallic and Al_2O_3-coated intermetallic samples is provided in Table 3. Seven samples of each of the uncoated and coated materials were tested to obtain the Weibull distribution parameters. A combined plot of the Weibull strength distribution of the uncoated and coated itermetallic substrates is shown in Fig. 2. It is important to note here that a quantitative comparison of the strengths of the samples with two different coating thicknesses should not be done, since the volume fractions of the coatings in the two cases are significantly different. While the average volume fraction of the Al_2O_3 coating is 5.3% for the samples with the 0.1 mm Al_2O_3 coating, it is 36.6% for the samples with the 1 mm Al_2O_3 coating. If the strength of the samples is corrected for the coating volume fraction, we find that the experimentally measured strength values of the 1 mm Al_2O_3-coated samples are in close agreement with those predicted theoretically. Furthermore, the dimensions and test ratios (test span to specimen thickness, test span to specimen width, etc.) are also very different for samples with the different Al_2O_3 coating thicknesses, which further eliminates any data comparison. However, it is reasonable to compare the strength values of the 0.1 mm Al_2O_3-coated samples with the strength of the uncoated intermetallic samples, since the test variables are very similar and the volume fraction of the 0.1 mm Al_2O_3 coating is small.

The strength of the uncoated intermetallic substrate was narrowly distributed, as evidenced by the relatively high Weibull modulus. The coefficient of variation was also within an acceptable range of what one can expect when testing brittle materials. The Weibull modulus and average strength of the 0.1 mm Al_2O_3-coated samples were very similar to those of the uncoated samples, indicating that the 0.1 mm Al_2O_3 coating did not adversely affect the strength of the intermetallic substrate (Al_2O_3 has a lower strength than Ti-25Al-10Nb-3V-1Mo). The coefficient of variation and correlation coefficients of the uncoated intermetallic and 0.1 mm Al_2O_3-coated intermetallic were also very similar.

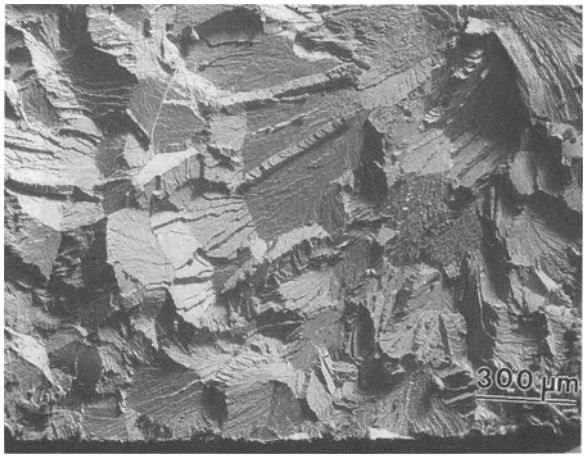

(a)

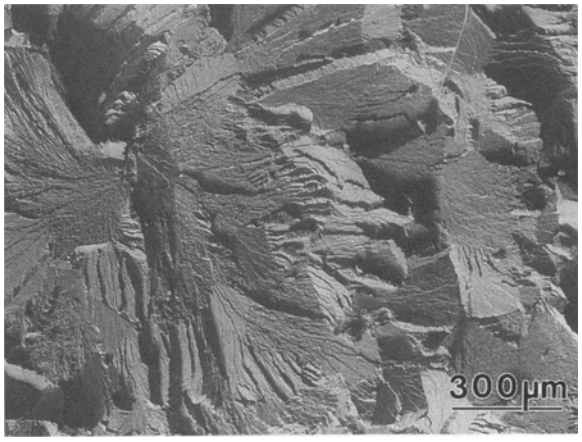

(b)

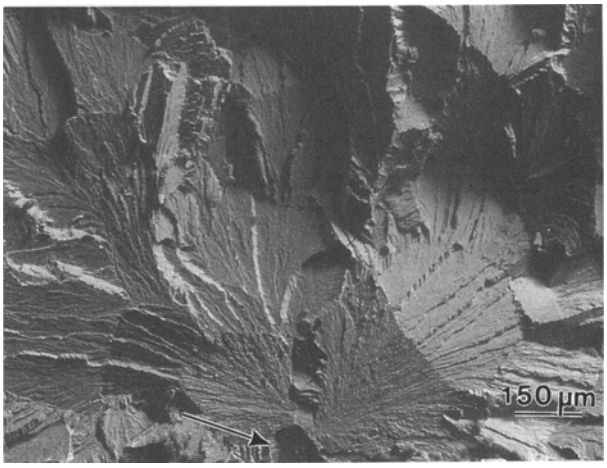

(c)

Fig. 4 Fracture surfaces of the uncoated intermetallic substrates. (a and b) General fracture characteristics with evidence of cleavage failure. (c) Origin of a flaw on the tensile surface of the bend sample (denoted by an arrow)

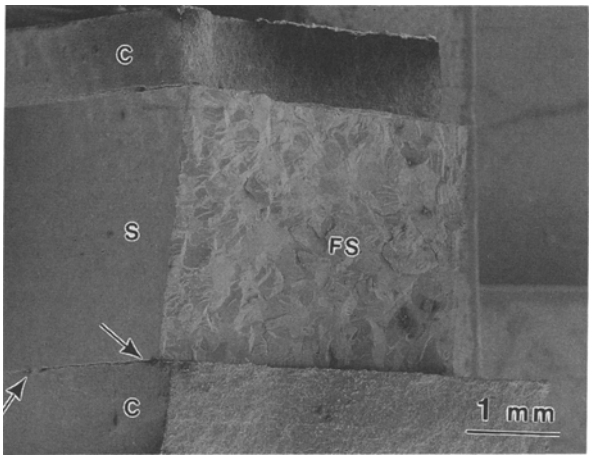

(a)

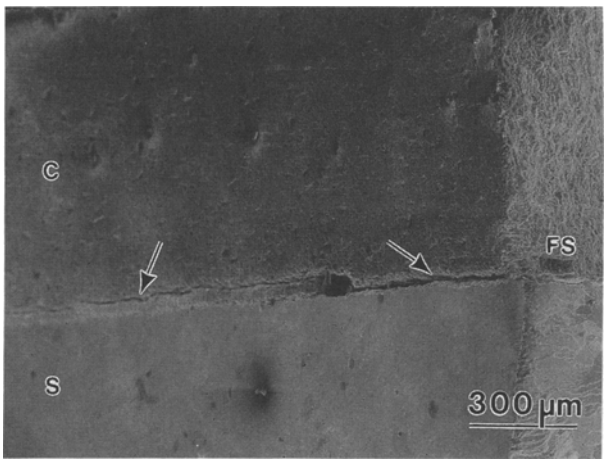

(b)

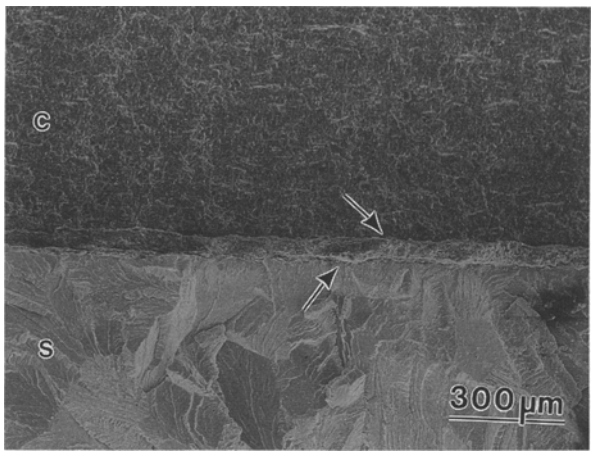

(c)

Fig. 5 Fracture surfaces of the 1.0 mm Al_2O_3-coated samples. (a) Coating/substrate interface. (b and c) Debonding occurs within the Al_2O_3 coating in the vicinity of the interface. FS, fracture surface; C, Al_2O_3 coating; S, intermetallic substrate; arrows, regions of cracking

Although the average Weibull strength of the samples coated with 1 mm Al_2O_3 was expectedly lower than the strength of the uncoated and 0.1 mm Al_2O_3-coated samples, the strength values of the intermetallics were widely distributed, as evidenced by the relatively low Weibull modulus. The coefficient of variation of the strength data was significantly larger than that for the uncoated and 0.1 mm Al_2O_3-coated samples. The low Weibull modulus and correlation coefficient are indicative of a larger scatter in the strength of the samples.

The strength of the 1 mm Al_2O_3-coated intermetallic samples is lower than the strength of the uncoated intermetallic as a result of the lower intrinsic strength of the Al_2O_3 coating itself (as compared to the strength of Ti-25Al-10Nb-3V-1Mo). The strength of the 1 mm Al_2O_3 coating is reduced by the porosity introduced in the coating during the plasma spraying process. The porosity in the coating is also responsible for the wide distribution in the strength of the 1 mm Al_2O_3-coated samples. Pores in the coating act as stress concentration sites, and help link propagating cracks. The porosity value for the 1 mm Al_2O_3 coating, 7.8%, is almost twice the porosity value for the 01. mm Al_2O_3 coating, 4.3%. The higher porosity is reflected in the lower strength and wider strength distribution of the 1 mm Al_2O_3-coated intermetallic system. For the 0.1 mm Al_2O_3 coating, the volume fractions of the coating and porosity in the coating are small, and they do not significantly affect the strength distribution of the intermetallic substrate.

A schematic of the load-displacement curves for the uncoated and coated intermetallic substrates can be seen in Fig. 3. The uncoated intermetallic samples exhibited characteristic linear elastic behavior to failure. Very little plasticity accompanied the failure process. The loading response for the 1.0 mm Al_2O_3-coated intermetallic samples exhibited two discontinuities. These discontinuities were attributed to the failure of the Al_2O_3 coating on the tensile and compression surfaces of the sample. On the other hand, such discontinuities were not observed in the case of the 0.1 mm Al_2O_3-coated samples. It is possible that the signal associated with the failure of the coating was not detected by the load cell, as a result of the small thickness of the coating itself.

Fractography of the coated and uncoated materials was carried out to determine the fracture characteristics of the different samples. Fracture surfaces of the uncoated intermetallic samples can be seen in Fig. 4. Failure in the uncoated intermetallic samples was initiated by flaws on the tensile surface of the sample (Fig. 4a). The cracks, once initiated, propagated rapidly through the interior of the sample. Fracture of the sample was of a "cleavage" type, as can be seen from the topography of the grains in Fig. 4(b) and (c).

Failure in all the coated intermetallic systems (Fig. 5, 6) was initiated by failure of the coating on the tensile surface. This in turn initiated a flaw at the coating/substrate interface, which eventually propagated through the intermetallic and led to subsequent failure of the system as a whole. Also, for the samples coated with 1.0 mm Al_2O_3 coating, transverse cracks were observed to form in the alumina coating, adjacent to the interface. These cracks formed in a region of the coating in close vicinity to the region where we had earlier observed cracks to form in our thermal cycling experiments (Ref 1). We attribute this cracking to the presence of flaws (microcracks) in that portion

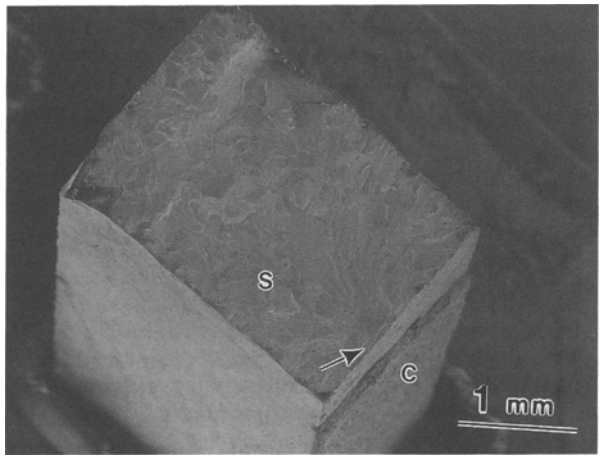

(a)

(b)

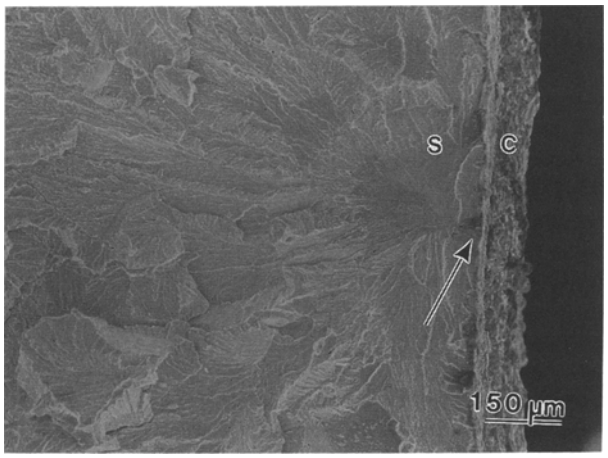

(c)

Fig. 6 Fracture surfaces of the 0.1 mm Al_2O_3-coated samples. (a) Coating/substrate interface. (b) Coating in the vicinity of the primary crack plane has spalled off. (c) Origin of the matrix flaw at the coating/matrix interface. FS, fracture surface; C, Al_2O_3 coating; S, intermetallic substrate; arrows, planes of debonding

of the coating. These microcracks are possibly the result of the spraying process, which was done in layers in order to obtain the thickness of 1.0 mm. Variation in the expansion and contraction occurring between the layers, during the plasma spraying operation, can lead to microcracking. Some coating material was found to remain adhering to the intermetallic substrate. This is because of the tortuosity of the interface and accompanying enhancement in the coating/substrate mechanical bonding from the shot blasting process performed on the intermetallic substrates prior to plasma spraying.

Some coating/matrix debonding was observed in samples with both the thick and thin coatings, but the extent of debonding was limited to a very small region in the vicinity of the primary crack plane. The coating in the vicinity of the primary crack plane also spalled off for samples with the 0.1 mm Al_2O_3 coating. No cracks were detected within th 0.1 mm Al_2O_3 coating itself. On the other hand, the 1.0 mm Al_2O_3 coating was left intact on the tensile and compressive sides of the bend samples.

Experimentally measured Young's modulus and damping values for the uncoated and coated intermetallic samples are given in Table 4. The strain amplitude for these measurements was near 10^{-7}. The Young's modulus of the intermetallic substrate as determined by us was slightly lower than the values in the literature (Table 1) but was well within the acceptable range for this material. We wanted to compare the experimentally determined Young's modulus of the coated intermetallic substrates with the theoretically predicted values. The theoretical values of the Young's modulus were calculated by using the rule of mixtures as:

$$E_{cs} = E_s V_s + E_c V_c \quad \text{(Eq 9)}$$

Here, E is the Young's modulus, V is the volume fraction, and the subscripts cs, s, and c refer to the coated intermetallic substrate, substrate, and coating, respectively. A correction is required to be applied for the value of E_c because of the porosity present in the Al_2O_3 coating. The porosity correction for the Young's modulus of the Al_2O_3 coating was obtained using MacKenzies' equation (Ref 6) as:

$$E_c = E_0(1 - 1 \cdot g\,\delta + o \cdot g\,\delta^2) \quad \text{(Eq 10)}$$

Here, E_0 is the modulus of the coating containing zero porosity (equal to 230 GPa) and ρ is the volume fraction porosity in the coating.

Using Eq 9 and 10, experimental data for the volume fraction and porosity, experimentally determined modulus for the substrate, and data for the modulus of Al_2O_3 from Table 1, we calculated the theoretical Young's modulus for the 0.1 mm Al_2O_3-coated intermetallic to be 121.6 GPa and the theoretical Young's modulus for the 1.0 mm Al_2O_3 to be 170.6 GPa.

Comparison of the experimental and theoretical results (Table 5) revealed a large discrepancy between the experimental and theoretical values of the Young's modulus of the 1.0 mm Al_2O_3-coated intermetallic substrate. The experimental value of the measured modulus was significantly lower than the modulus value predicted theoretically. This difference cannot be attributed to porosity in the coating, since that was already

Table 4 Measured Young's modulus (E) and damping (internal friction (Q^{-1})

Measurement	E, GPa	$Q^{-1} \times 10^{-3}$
Uncoated Ti25Al10Nb-31Mo		
1	111.1	0.4
2	112.2	0.4
3	112.4	0.5
4	111.2	1.3
5	112.3	0.3
Average	111.8	0.6
Standard deviation	0.63	0.43
0.1 mm Al_2O_3-coated Ti-25Al-10Nb-3V-1Mo		
1	113.5	1.3
2	113.7	1.8
3	112.9	2.8
4	113.5	1.7
5	114.0	0.9
Average	113.5	1.7
Standard deviation	0.4	0.71
1.0 mm Al_2O_3-coated Ti-25Al-10Nb-3V-1Mo		
1	113.9	4.0
2	113.4	6.0
3	113.5	5.6
4	114.9	2.0
5	114.1	6.3
Average	114.0	4.8
Standard deviation	0.62	1.78

accounted for in the calculations. The only other viable explanation is the presence of microcracks in the coating, formed either during the spraying process or during cooling down after plasma spraying. Microcracks present in the coating would lead to a substantial decrease in the measured Young's modulus (Ref 7).

The large damping values of the 1.0 mm Al_2O_3-coated intermetallic are further indication of the presence of microcracks in the coating, though part of the increase in the damping values of the coated intermetallic is a result of porosity in the coating. Studies have been done (Ref 8) to determine the effect of porosity on the damping of polycrystalline Al_2O_3. The damping values reported for Al_2O_3 ($0.08\text{-}0.12 \times 10^{-3}$) have been significantly lower than those measured for the intermetallic substrate. The experimentally measured damping values for the coated intermetallic substrates are up to 8 times larger than those of the uncoated intermetallic substrates and up to 40 times larger than that of the ceramic coating. Irrespective of the way in which the damping values of the two components (substrate and coating) are combined for the coated intermetallic, the experimentally determined values are still too large to be explained on the basis of contributions from each component of the coated system. However, any discontinuities at the coating/substrate interface and microcracks in the coating could increase the damping.

Table 5 Comparison of the experimentally determined values of Young's modulus (E) with those calculated theoretically

Sample condition	$E_{theoretical}$, GPa	$E_{experimental}$, GPa
Uncoated intermetallic	...	111.8
0.1 mm Al_2O_3-coated intermetallic	121.6	113.5
1.0 mm Al_2O_3-coated intermetallic	170.6	114

On the other hand, the experimentally determined Young's modulus of the 0.1 mm Al_2O_3-coated specimens is in close agreement with the theoretically predicted value. The damping values of the coated intermetallic are also similar to those of the uncoated substrate.

5. Conclusion

Our study has demonstrated the effect of the Al_2O_3 coating thickness on the bend strength, elastic modulus, and damping of the Ti-25Al-10Nb-3V-1Mo intermetallic substrate. The 1.0 mm thick coating increased the scatter in the strength of the coated intermetallic substrate. The Young's modulus of the samples coated with 1.0 mm thick Al_2O_3 was not much different from the modulus of the uncoated substrate, and it was significantly lower than the theoretically predicted value. The damping values of the 1.0 mm thick Al_2O_3-coated samples were significantly higher than those of the uncoated intermetallic substrate. Both of these variations were attributed to the presence of defects within the coating. The experimentally measured Young's modulus of the intermetallic samples coated with 0.1 mm thick Al_2O_3 was close to the value predicted theoretically. The damping values were also very similar to those of the uncoated intermetallic substrate. Hence, we can conclude that the 0.1 mm coating provides the required oxidation protection to the substrate without adversely affecting mechanical properties of the substrate.

References

1. R.U. Vaidya, Y.W. Sin, K.N. Subramanian, A.K. Zurek, and R. Castro, in *Processing and Fabrication of Advanced Materials*, TMS, 1993
2. R.U. Vaidya, A. Wolfenden, A.K. Zurek, S.L. Hosman, R. Castro, and K.N. Subramanian, *J. Adv. Mater.*, Vol 26 (No. 1), 1994, p 16
3. W.A. Weibull, *J. Appl. Mech.*, Vol 18 (No. 3), 1951, p 293
4. A. Wolfenden and W.H. Robinson, *Scr. Metall.*, Vol 10, 1976, p 763
5. V. Thomas, A.J. Glacomin, and A. Wolfenden, *Rev. Sci. Instrum.*, Vol 64, 1993, p 492
6. J.K. MacKenzie, *Proc. Phys. Soc.*, Vol B63, 1950, p 2
7. D.A. Hoke, M.A. Meyers, L.W. Meyer, and G.T. Gray, *Metall. Trans. A*, Vol 23, 1992, p 77
8. W.J. Lee and E.D. Case, *J. Mater. Sci.*, Vol 25, 1990, p 5043